Environmental Science & Technology

Article

pubs.acs.org/est

Concurrent Separation of CO_2 and H_2O from Air by a Temperature-Vacuum Swing Adsorption/Desorption Cycle

Jan Andre Wurzbacher,[†,‡] Christoph Gebald,[†,‡,§] Nicolas Piatkowski,[†] and Aldo Steinfeld*[,†,∥]

[†]Department of Mechanical and Process Engineering, ETH Zurich, 8092 Zurich, Switzerland

[‡]Climeworks Ltd., 8005 Zurich, Switzerland

[§]EMPA Material Science and Technology, 8600 Dübendorf, Switzerland

[∥]Solar Technology Laboratory, Paul Scherrer Institute, 5232 Villigen, Switzerland

Supporting Information

ABSTRACT: A temperature-vacuum swing (TVS) cyclic process is applied to an amine-functionalized nanofibrilated cellulose sorbent to concurrently extract CO_2 and water vapor from ambient air. The promoting effect of the relative humidity on the CO_2 capture capacity and on the amount of coadsorbed water is quantified. The measured specific CO_2 capacities range from 0.32 to 0.65 mmol/g, and the corresponding specific H_2O capacities range from 0.87 to 4.76 mmol/g for adsorption temperatures varying between 10 and 30 °C and relative humidities varying between 20 and 80%. Desorption of CO_2 is achieved at 95 °C and 50 $mbar_{abs}$ without dilution by a purge gas, yielding a purity exceeding 94.4%. Sorbent stability and a closed mass balance for both H_2O and CO_2 are demonstrated for ten consecutive adsorption−desorption cycles. The specific energy requirements of the TVS process based on the measured H_2O and CO_2 capacities are estimated to be 12.5 kJ/mol_{CO2} of mechanical (pumping) work and between 493 and 640 kJ/mol_{CO2} of heat at below 100 °C, depending on the air relative humidity. For a targeted CO_2 capacity of 2 mmol/g, the heat requirement would be reduced to between 272 and 530 kJ/mol_{CO2}, depending strongly on the amount of coadsorbed water.

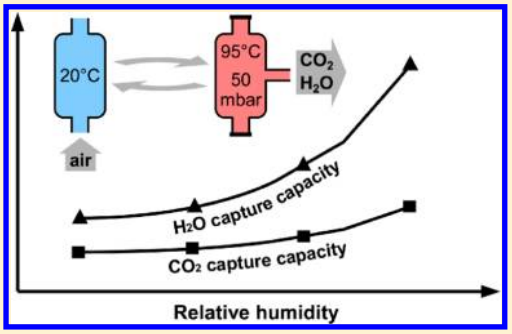

INTRODUCTION

Among several strategies to mitigate anthropogenic CO_2 emissions, capturing CO_2 directly from ambient air − usually referred to as direct air capture (DAC) − has recently attracted increasing interest.[1−12] The advantage of DAC is its ability to address present and past emissions from distributed and mobile sources, e.g., derived from the transportation sector. Furthermore, DAC systems need not be attached to the source of emission but can be logistically centralized and located next to the site of CO_2 storage/processing or of vast renewable (e.g., solar) energy resources. In particular, CO_2 extracted from the atmosphere can be processed to synthetic liquid hydrocarbon fuels using renewable energy in a closed material cycle.[13−15] Thereby, DAC uniquely offers the possibility of a truly sustainable liquid fuel-based energy future.[16,17] While some studies claim that DAC can potentially become competitive[5,18] and others question its economic feasibility,[19−21] it is evident that additional R&D on the fundamentals of DAC is required to reliably assess its ultimate industrial-scale applicability.

If, additionally, H_2O is coextracted from ambient air, major logistical benefits can be achieved in the production of synthetic liquid hydrocarbon fuels using concentrated solar energy.[13−15,22] Solar fuel production plants will be located in deserted regions of the earth's sunbelt with vast direct solar irradiation but limited or no fresh water resources. Water coextracted in a DAC process can thus become a valuable byproduct. Note that, if seawater is accessible, fresh water extraction via reverse osmosis desalination[23] is about 2 orders of magnitude more energy efficient than water extraction from air via adsorption.

Solid amine-functionalized materials have been identified as promising sorbents for DAC, as they offer relatively high specific CO_2 capacities and uptake rates under extremely low CO_2 partial pressures, such as in the case of ambient air.[7−10,12,24−30] The vast majority of previous studies on these materials focused on maximizing their CO_2 adsorption capacity, while sorbent regeneration was usually achieved by purging with an inert gas, yielding − again − highly diluted CO_2. Desorption of concentrated, high-purity CO_2 is evidently crucial for downstream applications, yet this issue remained mostly disregarded.[31] A few studies applied steam stripping,[32] moisture swing,[6] or temperature-vacuum swing (TVS)[11,33] processes to obtain concentrated CO_2 from the air.

Another intriguing advantage of amine-functionalized solid sorbents is their tolerance to air moisture.[12,31,34] In contrast to

Received: May 21, 2012
Revised: July 22, 2012
Accepted: July 23, 2012
Published: July 23, 2012

   dx.doi.org/10.1021/es301953k | Environ. Sci. Technol. 2012, 46, 9191−9198

physical sorbents such as zeolites, an increase of the CO_2 adsorption capacity was observed under humid conditions compared to dry conditions.[7,11,25,33,35] However, substantial amounts of water are coadsorbed from moist gases.[25,36] Formation of carbamates and carbamic acid was postulated as the main underlying CO_2 adsorption mechanism on amine-modified silica under dry and humid conditions.[37−40] Similar mechanisms were concluded for amine-modified cellulose.[28] Additional adsorption of H_2O presumably occurs through physical adsorption.[35]

As opposed to flue gases, the molar water content of air is typically 1−2 orders of magnitude higher than its CO_2 content. Thus, water adsorption per gram of sorbent material can substantially exceed CO_2 adsorption.[25,36] This in turn implies significant heat requirements for water desorption during sorbent regeneration. The required heat of water desorption will typically be of the same order of magnitude as the heat of evaporation of the coadsorbed water.[41] Corrosion and fouling due to condensed water vapor might also be of concern in an industrial large-scale implementation. Therefore, quantitative data on coadsorption of H_2O are important for the design of a DAC process based on a solid sorbent material.

Although several proposed DAC concepts are based on amine-functionalized materials, their coadsorption of water during CO_2 capture has hardly been quantified.[9,11,12] Data on H_2O adsorption on an amine-based sorbent was shown for spacecraft air regeneration without CO_2 concentration.[41] Water adsorption isotherms on amine-grafted pore expanded mesoporous silica gel were measured[36,42] but only for single component adsorption. Co-adsorption of CO_2 and H_2O on amine-functionalized silica was analyzed in column-breakthrough experiments, but no concentrated CO_2 was extracted.[25]

In a previous paper, we analyzed the TVS process applied to an amine-functionalized solid sorbent material.[33] The objective of the present paper is the detailed measurement of coadsorption of CO_2 and H_2O and the analysis of the effects of varying adsorption temperature and relative humidity (RH) of air. For this purpose we have designed an experimental setup that uses a membrane-based gas dryer to selectively extract the water vapor from the desorbed stream under vacuum conditions prior to its condensation, enabling an accurate mass balance. These measurements further enable a more reliable estimate of the energy requirements of the TVS process.

EXPERIMENTAL SECTION

Synthesis and Characterization. The sorbent material (APDES-NFC-FD) was obtained through a one-pot reaction of an aqueous suspension of nanofibrillated cellulose (NFC) and 3-aminopropylmethyldiethoxysilane (APDES) similar to a procedure described elsewhere.[28] Details of the synthesis and characterization are provided in the Supporting Information. The BET surface area of the APDES-NFC-FD sorbent material was 12.2 m^2/g. Its amine content was 3.86 $mmol_N/g$ sorbent.

Experimental Setup. The TVS adsorption/desorption cycles were performed on an experimental setup similar to a setup described elsewhere.[33] A packed bed of 10 g of sorbent material that was contained in a 45 mm × 45 mm rectangular reactor with an oil-filled jacket for cooling and heating was used for cyclic adsorption and desorption. The bed length of 80 mm was chosen to obtain a low pressure drop because a sharp breakthrough, which would require a larger bed length, was not relevant for this study. A detailed description and a schematic of the setup are contained in the Supporting Information.

All experiments used dried, technical-grade pressurized air for adsorption obtained by compressing ambient air with a CO_2 content varying between 400−510 ppm. By comparing several otherwise equal adsorption/desorption runs with different inlet CO_2 concentration, it was verified that this variation has negligible effect on the results (see Figure S2, Supporting Information). This can be explained with the relatively flat shape − far beyond the Henry's law regime − of the CO_2 adsorption isotherms of amine-modified porous adsorbents even at CO_2 concentrations of 400 ppm.[7]

To quantify the amount of H_2O desorbed under vacuum conditions, the gas flow exiting the reactor was passed through one channel of a Nafion membrane gas dryer (Perma Pure MD-070-72S) before entering the vacuum pump. Dried pressurized air, controlled by an electronic mass flow controller (Bronkhorst EL-FLOW), was passed through the other channel as a "drying gas" in counter-current flow configuration. The piping between the reactor and the gas dryer was heated to avoid condensation. Nearly all water vapor contained in the desorption gas diffused through the Nafion membrane into the drying gas, as corroborated by blank experiments. This amount of H_2O was quantified by measuring the RH of the drying gas at the exit of the channel with an electronic sensor (Vaisala HMP110).

For comparison, the CO_2 adsorption capacity for 10 h adsorption at 20 °C and 0/40% RH after N_2 purge desorption was measured on an experimental setup described elsewhere.[33]

Data Processing. The CO_2 and H_2O adsorbed during a single TVS cycle $\Delta q_{CO_2}^{(ads)}$ (mmol CO_2/g sorbent material) and $\Delta q_{H_2O}^{(ads)}$ (mmol H_2O/g sorbent material) are determined by integrating the breakthrough profiles

$$\Delta q_{CO_2/H_2O}^{(ads)} = \int_{t=0}^{t=t_{ads}} \frac{\dot{n}_{air}\cdot(c_{0,CO_2/H_2O} - c_{1,CO_2/H_2O})}{m_s} dt \quad (1)$$

where t_{ads} is the adsorption time, $\dot{n}_{air}$ is the molar flow rate of the air stream, $c_{0,CO_2/H_2O}$ and $c_{1,CO_2/H_2O}$ are the CO_2/H_2O concentrations at the inlet and outlet of the reactor, and m_s is the mass of the sorbent material contained in the reactor. The CO_2 desorbed during a single TVS cycle $\Delta q_{CO_2}^{(des)}$ (mmol CO_2/g) is determined by integrating over the desorption process

$$\Delta q_{CO_2}^{(des)} = \int_{t=0}^{t=t_{des}} \frac{\dot{n}_{CO_2}}{m_s} dt \quad (2)$$

where t_{des} is the desorption time, and $\dot{n}_{CO_2}$ is the measured molar flow rate of desorbed CO_2. The H_2O desorbed during a single TVS cycle $\Delta q_{H_2O}^{(des)}$ (mmol H_2O/g) is determined by integrating over the H_2O concentration profile in the drying gas stream at the exit of the membrane gas dryer

$$\Delta q_{H_2O}^{(des)} = \int_{t=0}^{t=t_{des}} \frac{\dot{n}_d\cdot c_{d,H_2O}}{m_s} dt \quad (3)$$

where $\dot{n}_d$ is the molar flow rate of the drying gas stream, and c_{d,H_2O} is the H_2O concentration in the drying gas leaving the gas dryer calculated from its RH, temperature, and pressure.

The baseline operational parameters of the adsorption/desorption experiments are listed in Table 1. These were varied for the purpose of evaluating the effects of adsorption

Table 1. Operational Parameters of the CO_2 and H_2O Adsorption/Desorption Experiments

parameter	
adsorption time (h)	5
desorption time (h)	1
adsorption flow rate (l_N/min)	4
adsorption temperature (°C)	10/20/30
adsorption relative humidity (% at adsorption temperature)	20/40/60/80
adsorption CO_2 concentration (ppm)	400−510
desorption temperature (°C)	95
desorption pressure (mbar)	50

temperature and RH. All other operational conditions, in particular those during desorption, were fixed. Each adsorption cycle started therefore from the same equilibrium baseline state of the sorbent material to facilitate comparison of the individual cycles with varying adsorption conditions. The adsorption time of 5 h was required to attain sufficient loading of the sorbent material but did not lead to full adsorption equilibrium. For each parameter combination, two adsorption/desorption cycles were performed to ensure reproducibility; the reported results represent the average of both cycles. All experiments use the same sorbent sample. Periodic repetitions of a standard cycle during the parametric study verified that no measurable degradation of the sample occurred.

RESULTS AND DISCUSSION

CO_2 and H_2O Adsorption/Desorption Capacities. The results of the TVS adsorption/desorption measurements are shown in Figure 1. The specific CO_2 and H_2O adsorption/desorption capacities are plotted as a function of the air RH for adsorption temperatures of 10, 20, and 30 °C. The RH was varied between 20 and 80% at 10 and 20 °C, and between 20 and 60% at 30 °C, to prevent condensation in the piping in the latter case. The CO_2 adsorption/desorption mass balance is well closed for all parameter combinations, with average deviation <2.5%. The corresponding H_2O mass balance exhibits discrepancy for some data points, caused by inaccuracies in the RH measurement during adsorption. Due to the relatively high water content of air compared to its CO_2 content, the H_2O adsorption measurement is more sensitive to small sensor deviations than the CO_2 measurement. Thus, the more accurate desorption values are used in the analysis that follows.

At 10 °C adsorption temperature, the CO_2 capacity increases from 0.36 mmol/g at 20% RH to 0.63 mmol/g at 80% RH, corresponding to amine efficiencies (moles CO_2 adsorbed per moles of amine groups) of 0.09 and 0.16, respectively. At 20 °C adsorption temperature, the CO_2 capacity varies from 0.39 mmol/g at 20% RH to 0.65 mmol/g at 80% RH. At 30 °C, it varies from 0.32 mmol/g at 20% RH to 0.50 mmol/g at 60% RH. The amine efficiencies are lower than reported elsewhere, because (i) the adsorption process was stopped after 5 h before attainment of the complete full capacity, and (ii) desorption under TVS conditions, while resulting in a stream of concentrated CO_2, is known to yield lower capacities than desorption under inert purge gas, which results in a stream of diluted CO_2.[33] The purity of the desorbed CO_2 for all data points was between 94.4% and 96.7%. The corresponding H_2O capacity at 10 °C adsorption temperature increases from 0.87 mmol/g at 20% RH to 4.20 mmol/g at 80% RH. At 20 °C adsorption temperature, the H_2O capacity increases from 0.94 at 20% RH to 4.76 mmol/g at 80% RH. At 30 °C, it increases from 0.96 at 20% RH to 3.02 mmol/g at 60% RH.

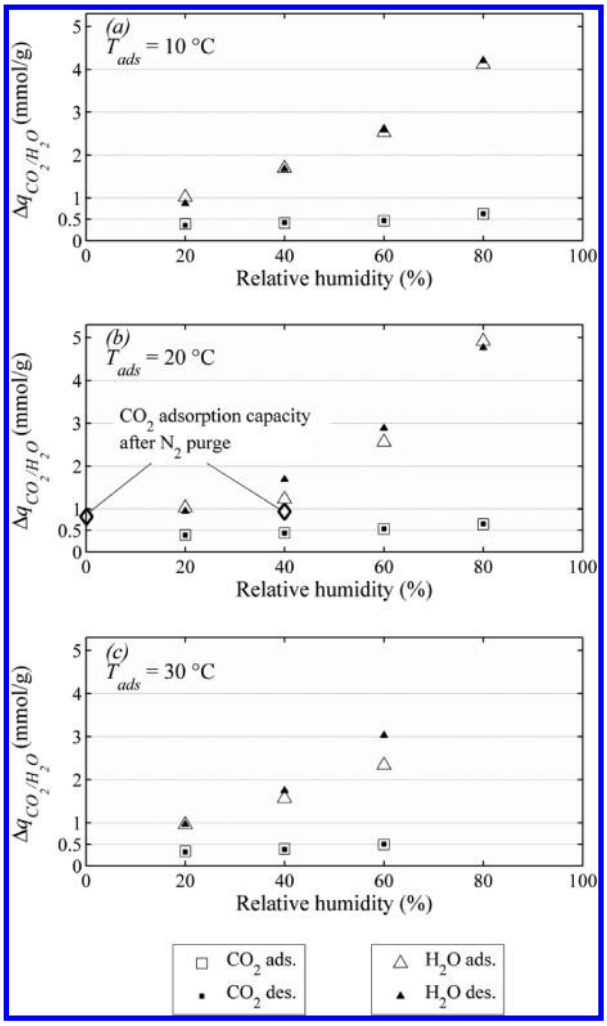

Figure 1. Specific CO_2 and H_2O adsorption/desorption capacities of APDES-NFC-FD in the TVS cyclic process as a function of the air relative humidity for adsorption temperatures of 10 °C (a), 20 °C (b), and 30 °C (c).

For the purpose of comparison with published data, Figure 1b contains in addition the values of the adsorption capacities of 0.82 and 0.94 mmol/g measured for 10 h adsorption at 0 and 40% RH, respectively, after N_2 purge desorption.

Evidently, the measurements reveal a strong promoting effect of the RH during adsorption on both CO_2 and H_2O capacities for all investigated adsorption temperatures. The influence is larger on H_2O adsorption than on CO_2 adsorption. For example, the H_2O capacity increases by a factor of 5, while the CO_2 capacity increases by a factor of 1.7 when the RH varies from 20% to 80% at 20 °C adsorption temperature. These results are in agreement with the generally known promoting effect of humidity on CO_2 adsorption on amine-functionalized solid sorbent materials.[31,34] The fact that a higher level of RH leads to a stronger increase of the CO_2 capacity has been previously observed.[25,36,43] H_2O coadsorption of 4.7 and 7.29 mmol/g was observed for 27% and 64% RH, respectively, on amine functionalized mesoporous silica that was regenerated by purging inert gas.[25] Our results quantify for the first time the promoting effect of the RH of air on the coadsorption/

dx.doi.org/10.1021/es301953k | Environ. Sci. Technol. 2012, 46, 9191−9198

desorption capacities of CO_2 and H_2O for the TVS process extracting pure CO_2 from air.

While the detailed mechanisms of binary adsorption of CO_2 and H_2O are not yet fully understood, hydrogen bonding with the surface functional groups and multilayer adsorption have been proposed as general mechanisms for the coadsorption of H_2O and CO_2 on porous sorbent materials.[44] On cellulose fibrils, H_2O molecules are assumed to mainly adsorb in multilayers on the cellulose hydroxyl surface groups.[45] Besides the chemical interaction of H_2O and CO_2 with the surface functionalities, the smaller van der Waals diameter of H_2O molecules compared to that of CO_2 molecules[44] can be one reason for the observed H_2O capacities largely exceeding the corresponding CO_2 capacities. Moreover, multilayer adsorption of H_2O is presumably responsible for the stronger increase of the H_2O capacity with RH vis-à-vis that of the CO_2 capacity.

The TVS adsorption/desorption CO_2 capacities achieved in this study for an amine-functionalized nanofibrilated cellulose sorbent are about twice higher than those obtained previously for an amine-functionalized silica gel sorbent,[33] while adsorption time was only 5 h instead of 24 h. This is associated with the higher amine content of the APDES-NFC-FD sorbent used in this study and its more favorable adsorption kinetics.[28] In another TVS study, a CO_2 capacity of 0.13 mmol/g under moist conditions was reported for an amine-grafted silica sorbent.[11]

From Figure 1 and Figure S3 in the Supporting Information, which shows the capacities as a function of the adsorption temperature, it can be seen that the influence of the adsorption temperature on the CO_2/H_2O capacities at fixed RH is minor. For example, the CO_2 capacities for adsorption temperatures of 10, 20, and 30 °C at a fixed 40% RH are 0.42, 0.44, and 0.38 mmol/g, respectively. The corresponding H_2O capacities are 1.67, 1.69, and 1.74 mmol/g, respectively. Since the RH at different adsorption temperatures does not reflect the absolute water content of the air, the measured capacities are also plotted as a function of the partial pressure of H_2O in Figure 2. For clarity, only the desorption values are shown. It becomes evident that, at constant H_2O partial pressure, both CO_2 and H_2O capacities strongly decrease with increasing adsorption temperature. For example, at a partial H_2O pressure of about 9 mbar, the H_2O capacities at 10, 20, and 30 °C are 4.20, 1.69, and 0.96 mmol/g, respectively. The corresponding CO_2 capacities are 0.63, 0.44, and 0.32 mmol/g, respectively. This coherence is a direct consequence of the relation between the three variables H_2O partial pressure, temperature, and RH, of which only two are independent and the respective third one can be calculated from the corresponding vapor pressure of H_2O.

Therefore, describing the H_2O/CO_2 capacities as a function of the relative humidity turns out to be most convenient, since this representation is nearly independent of the adsorption temperature in the temperature range considered in this study. This is in agreement with other studies in which water adsorption was observed to be only marginally influenced by temperature at constant RH.[46,47] In fact, both the strong temperature dependence of the adsorption capacities at constant H_2O partial pressure (Figure 2) and the negligible dependence at constant RH are predicted from thermodynamic principles. According to the Clausius−Clapeyron equation, the temperature dependence of the adsorption capacity scales with the isosteric heat of adsorption. As shown elsewhere,[48] when the H_2O capacity is expressed as a function of H_2O partial pressure, the corresponding isosteric heat of adsorption to be used for the evaluation of the Clausius−Clapeyron equation is the total heat of adsorption, i.e. the sum of the "net" heat of adsorption and the latent heat of evaporation. On the other hand, when the H_2O capacity is expressed as a function of RH, the Clausius−Clapeyron equation needs to be evaluated by using the "net" heat of adsorption only. The latter is relatively small, since the heat of adsorption for amine modified sorbent materials is known to approach the value of the heat of H_2O evaporation.[41]

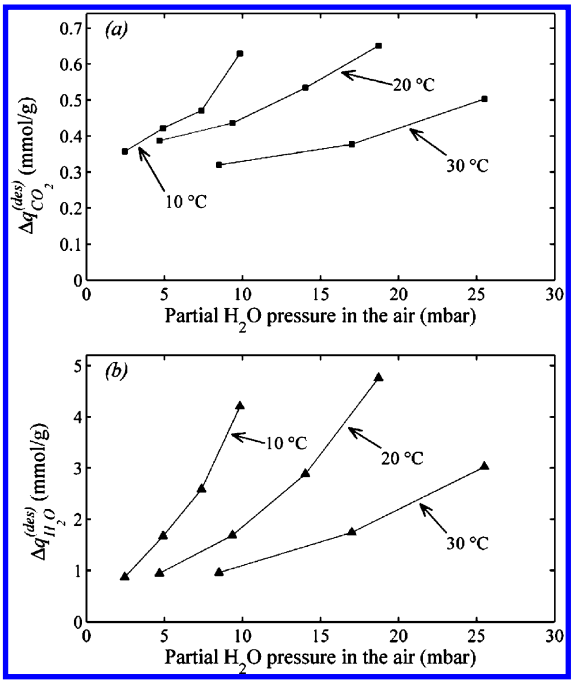

Figure 2. Specific CO_2 (a) and H_2O (b) desorption capacities in a TVS cyclic process as a function of the H_2O partial pressure for adsorption temperatures of 10, 20, and 30 °C.

While thermodynamics predict a marginal decrease of the CO_2/H_2O capacities with increasing temperature, the observed minimal increase for several data points (Figure S3, Supporting Information) is attributed to − besides measurement uncertainty − the nonideal behavior of the binary CO_2/H_2O system.[44] For the CO_2 capacities, further overlapping of equilibrium and kinetic effects is likely.

To compare the rates of CO_2 and H_2O adsorption, the breakthrough curves at 20 °C adsorption temperature and 40% RH are shown in Figure 3. Breakthrough of water occurs much faster than that of CO_2, which is consistent with previous results obtained with diluted CO_2 streams.[25] After approx-

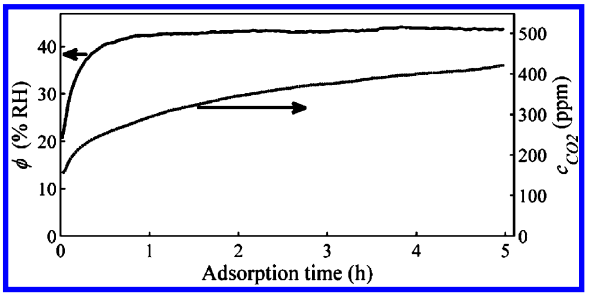

Figure 3. CO_2 and H_2O adsorption breakthrough curves at 20 °C adsorption temperature and 40% RH.

dx.doi.org/10.1021/es301953k | Environ. Sci. Technol. 2012, 46, 9191−9198

imately 1 h, H_2O adsorption reaches completion, while CO_2 adsorption does not reach equilibrium within 5 h adsorption time. Thus, longer adsorption times yield higher CO_2 to H_2O adsorption ratios for a DAC process. This is confirmed by Figure 4, which shows the cumulative CO_2 and H_2O uptakes

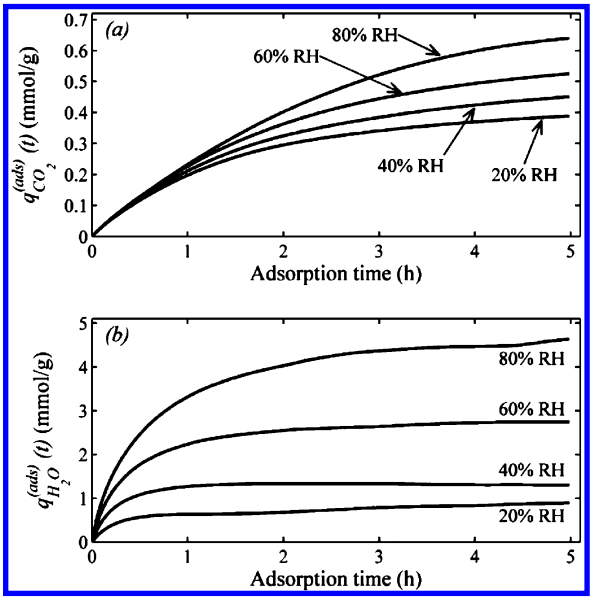

Figure 4. CO_2 (a) and H_2O (b) uptake during adsorption at an adsorption temperature of 20 °C and an air relative humidity of 20, 40, 60, and 80%.

over the adsorption process for 20 °C adsorption temperature and various RH. After 5 h adsorption time, the CO_2 uptake curves are still considerably increasing, while the corresponding H_2O curves have reached a constant plateau for all RH values. Slight variations are due to sensor deviations. Further, the CO_2 uptake curves exhibit the same profile for all RH levels, indicating the same underlying rate controlling mechanism determined presumably by diffusion and surface reaction with the amine groups.

Multicycle Experiment. The stability of the material and repeatability of the measurements are examined by performing 10 equal, consecutive adsorption/desorption cycles. The adsorption temperature and RH were fixed at 20 °C and 40%, respectively. The measured CO_2 and H_2O adsorption/desorption capacities for each cycle are shown in Figure 5. The CO_2 adsorption/desorption values remain stable over all cycles, and the corresponding mass balance is accurately closed. The average adsorbed and desorbed amounts of CO_2 are 0.415 mmol/g and 0.421 mmol/g, respectively. The amount of desorbed H_2O also remains stable with an average of 1.73 mmol/g. The water adsorption/desorption mass balance is well closed for cycles 3, 4, 5, 8, and 9. For the other cycles, discrepancy is associated with the sensitivity of the H_2O adsorption measurement to small drifts in the RH measurements.

Energy Requirement. The influence of the adsorption conditions on the energy consumption of a TVS process is estimated based on the experimentally measured capacities. The mechanical compression work of desorbed CO_2, heat of desorption of CO_2 and H_2O, and heat for the thermal swing of the sorbent material and adsorbed species are considered. The heat capacities of the adsorbed species CO_2 and H_2O were approximated by the pure component heat capacities of gaseous CO_2 and liquid H_2O, respectively. Parasitic losses such as pressure drops across pipes, heat losses, and heat transfer irreversibilities are omitted from consideration. The molar amount of desorbed water per mole of desorbed CO_2 is the ratio of the measured values in this work. The assumptions are summarized in Table S1 (Supporting Information).

The energy requirement for sorbent regeneration in the TVS process is given by the electrical input for operating the vacuum pump (eq 4), the heat input for bringing the sorbent material to the desorption temperature (eq 5), and the heat input for the desorption enthalpies of CO_2 and H_2O (eq 6).[33] The specific sensible heat, heat of desorption, and total required heat in kJ

Table 2. Heat Requirements for Sorbent Regeneration at Various Adsorption Temperatures and Relative Humidity

T_{ads} (°C)	ϕ (% RH)	Q_{sens} (kJ/mol$_{CO2}$)	Q_{des} (kJ/mol$_{CO2}$)	$Q = Q_{sens} + Q_{des}$ (kJ/mol$_{CO2}$)
10	20	352	205	**557**
10	40	311	276	**588**
10	60	291	348	**639**
10	80	236	404	**640**
20	20	288	205	**493**
20	40	266	272	**538**
20	60	230	344	**575**
20	80	206	434	**639**
30	20	302	231	**532**
30	40	267	308	**575**
30	60	213	373	**586**

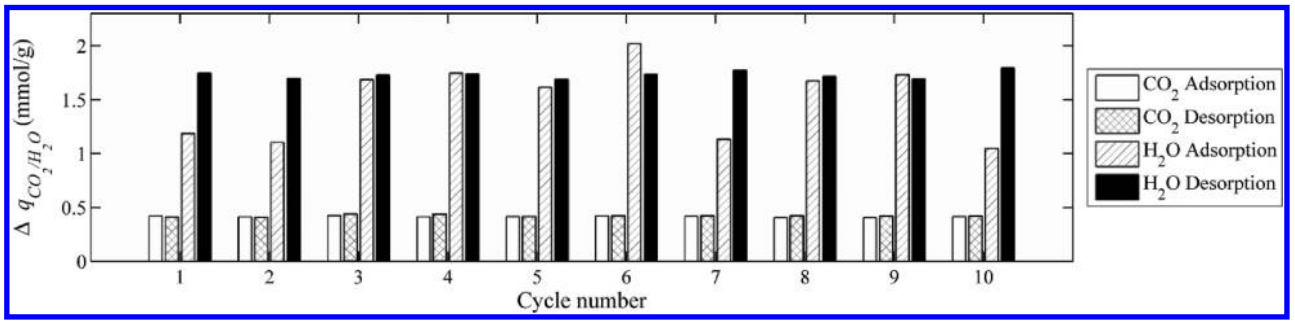

Figure 5. Specific adsorbed/desorbed amounts of CO_2 and H_2O in multicycle experiment at an adsorption temperature of 20 °C and an air relative humidity of 40%.

dx.doi.org/10.1021/es301953k | Environ. Sci. Technol. 2012, 46, 9191−9198

per mole of CO_2 separated are shown in Table 2 for 10, 20, and 30 °C adsorption temperatures and 20, 40, 60, and 80% RH.

$$W_{comp} = \frac{1}{\eta_{pump}} \cdot R \cdot T_{pump} \cdot \ln\left(\frac{p_{amb}}{p_{des}}\right) \quad (4)$$

$$Q_{sens} = \left(\frac{1}{\Delta q_{CO_2}^{(des)}} \cdot c_{p,sorb} + c_{p,CO_2} + \frac{\Delta q_{H_2O}^{(des)}}{\Delta q_{CO_2}^{(des)}} \cdot c_{p,H_2O}\right) \cdot (T_{des} - T_{ads}) \quad (5)$$

$$Q_{des} = h_{des,CO_2} + \frac{\Delta q_{H_2O}^{(des)}}{\Delta q_{CO_2}^{(des)}} \cdot h_{des,H_2O} \quad (6)$$

For example, at 20 °C adsorption temperature and 20% RH, the measured amounts of desorbed CO_2 and H_2O are 0.39 mmol/g and 0.94 mmol/g, respectively, and the corresponding required total heat is 493 kJ/mol_{CO2}. On the other hand, increasing the RH to 80% while keeping all other parameters results in an increase in the amount of desorbed CO_2 and H_2O to 0.65 mmol/g and 4.76 mmol/g, respectively, while the corresponding required heat is increased to 639 kJ/mol_{CO2}. The required mechanical work for the vacuum pump is 12.5 kJ/mol_{CO2} for all cases. Thus, although a higher RH significantly promotes CO_2 adsorption and, consequently, reduces the mass of the sorbent material per mole of adsorbed CO_2 and the corresponding sensible heat input, the overall heat consumption may still increase with RH due to disproportionately higher coadsorption of H_2O and the corresponding heat of desorption. Therefore, unless increased water adsorption is explicitly desired despite the associated energy penalty – e.g., when a source of fresh water such as that obtained via reverse osmosis desalination of seawater is unavailable – it will be more favorable to operate the DAC system in air with low RH. In contrast, the effect of the adsorption temperature on the energy consumption is less pronounced. For example, the total required heats for a TVS at 10 and 30 °C adsorption temperatures and 40% RH are 588 kJ/mol_{CO2} and 575 kJ/mol_{CO2}, respectively. These effects have evidently an impact on the economic viability of the DAC process, especially when evaluating the costs of the sorbent material and the energy requirements.

Figure 6 shows the requirements of heat at below 100 °C of the TVS process as a function of the specific CO_2 adsorption/desorption capacity varying between 0.5 mmol/g (experimentally verified in this study) to 2 mmol/g (targeted for an optimized sorbent). The adsorption temperature is 20 °C. The specific H_2O capacity is assumed to be 2.4, 3.9, 5.4, and 7.3 times that of CO_2 as measured in this work for 20, 40, 60, and 80% RH, respectively. At a H_2O:CO_2 capacity ratio of 2.4, the heat requirement decreases from 429 to 272 kJ/mol_{CO2} when the specific CO_2 capacity increases by a factor of 4 from 0.5 to 2 mmol/g. At a H_2O:CO_2 capacity ratio of 7.3, it decreases from 687 to 530 kJ/mol_{CO2}. The required mechanical work remains constant at 12.5 kJ/mol_{CO2} for all cases. A higher CO_2 capacity beyond 2 mmol/g results in an ever decreasing heat requirement because the contribution of the sensible heat term becomes less significant. On the other hand, the influence of the specific H_2O capacity on the heat requirement is much larger, which again justifies its accurate quantification as accomplished in this study.

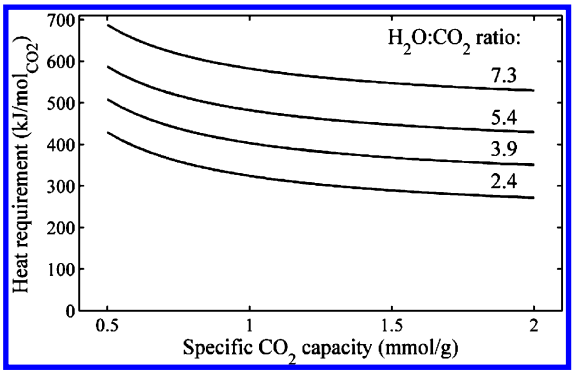

Figure 6. Requirement of heat at below 100 °C of the TVS process as a function of the specific CO_2 adsorption/desorption capacity, for the measured H_2O:CO_2 capacity ratios at 20 °C adsorption temperature.

■ ENVIRONMENTAL IMPLICATIONS

The sorbent material examined in this study is based on cellulose as solid support. This minimizes the environmental impact of large-scale manufacturing as it uses a natural, abundant, renewable feedstock. Evidently, the full advantage of such a renewable-based support is achieved provided its adsorption capacity is comparable to that of conventional sorbent materials based on nonrenewable supports. The quantification of adsorbed/desorbed CO_2 and H_2O allows for a more accurate estimation of the specific energy requirements of the TVS process and, consequently, its viability for future industrial implementation.

The separation of CO_2 from atmospheric air in combination with its processing to synthetic liquid hydrocarbon fuels with solar energy[13−15,22] can significantly contribute toward mitigation of anthropogenic greenhouse gas emissions in the transportation sector. Especially for the case of CO_2-neutral aviation fuels, this approach can overcome sustainability limitations of biofuels while avoiding the inherent restrictions associated with other alternative fuels, such as H_2, that require major changes in aircraft design and infrastructure. Ultimately, combining DAC that concurrently separates CO_2 and H_2O with the solar conversion of CO_2 and H_2O into liquid fuels may reduce energy requirements and costs by avoiding long-range transportation of CO_2 and eliminating the use of fresh water resources as well as driving the DAC process with waste heat recuperated from the solar process.

■ ASSOCIATED CONTENT

Supporting Information

Material synthesis and characterization; description and schematic of experimental setup; figures; table with assumptions. This material is available free of charge via the Internet at http://pubs.acs.org.

■ AUTHOR INFORMATION

Corresponding Author

*Phone: +41-44-6327929. Fax: +41-44-6321065. E-mail: aldo.steinfeld@ethz.ch.

Notes

The authors declare no competing financial interest.

■ ACKNOWLEDGMENTS

This work has been conducted in the framework of a joint project of ETH Zurich, the Swiss Federal Laboratories for

Materials Science and Technology (Empa), and the ETH Spin-off company Climeworks Ltd. The project partners thank Gebert Ruef Foundation for financial support.

NOMENCLATURE

$c_{0,CO_2/H_2O}$	CO_2/H_2O concentration upstream of the adsorption reactor
$c_{1,CO_2/H_2O}$	CO_2/H_2O concentration downstream of the adsorption reactor
c_{d,H_2O}	H_2O concentration in the drying gas at the exit of the gas dryer
$c_{p,sorb}$	heat capacity of the sorbent material
c_{p,CO_2}	heat capacity of adsorbed CO_2
c_{p,H_2O}	heat capacity of adsorbed H_2O
h_{des,CO_2}	heat of CO_2 desorption
h_{des,H_2O}	heat of H_2O desorption
m_s	mass of the sorbent material sample
$\dot{n}_{air}$	molar flow rate of air
$\dot{n}_{CO_2}$	molar flow rate of CO_2
$\dot{n}_d$	molar flow rate of drying gas (air)
p_{amb}	ambient pressure
p_{des}	desorption pressure
$q^{(ads)}_{CO_2/H_2O}(t)$	cumulative CO_2/H_2O uptake during adsorption
$\Delta q^{(ads)}_{CO_2/H_2O}$	cyclic CO_2/H_2O adsorption capacity in TVS process
$\Delta q^{(des)}_{CO_2/H_2O}$	cyclic CO_2/H_2O desorption capacity in TVS process
Q	total heat requirement for sorbent regeneration
Q_{des}	total heat of desorption
Q_{sens}	sensible heat required to heat up sorbent material for desorption
R	ideal gas constant
t	time
T	temperature
T_{pump}	operating temperature of the vacuum pump
W_{comp}	mechanical compression work
η_{pump}	efficiency of the vacuum pump
ϕ	relative humidity

Subscripts

ads adsorption
des desorption

Acronyms

APDES	3-aminopropylmethyldiethoxysilane
APDES-NFC-FD	sorbent material used in this study
DAC	direct air capture of CO_2
NFC	nanofibrillated cellulose
RH	relative humidity
TVS	temperature-vacuum swing

REFERENCES

(1) Jones, C. W. CO2 Capture from dilute gases as a component of modern global carbon management. *Ann. Rev. Chem. Biomol. Eng.* **2011**, *2*, 2.1−2.22, DOI: 10.1146/annurev-chembioeng-061010-114252.

(2) Keith, D. W. Why capture CO2 from the atmosphere? *Science* **2009**, *325* (5948), 1654−1655, DOI: 10.1126/science.1175680.

(3) Mahmoudkhani, M.; Keith, D. W. Low-energy sodium hydroxide recovery for CO2 capture from atmospheric air-thermodynamic analysis. *Int. J. Greenhouse Gas Control* **2009**, *3* (4), 376−384, DOI: 10.1016/j.ijggc.2009.02.003.

(4) Nikulshina, V.; Gebald, C.; Steinfeld, A. CO2 capture from atmospheric air via consecutive CaO-carbonation and CaCO3-calcination cycles in a fluidized-bed solar reactor. *Chem. Eng. J.* **2009**, *146* (2), 244−248, DOI: 10.1016/j.cej.2008.06.005.

(5) Lackner, K. S. Capture of carbon dioxide from ambient air. *Eur. Phys. J. Special Topics* **2009**, *176*, 93−106, DOI: 10.1140/epjst/e2009-01150-3.

(6) Wang, T.; Lackner, K. S.; Wright, A. Moisture swing sorbent for carbon dioxide capture from ambient air. *Environ. Sci. Technol.* **2011**, *45* (15), 6670−6675, DOI: 10.1021/Es201180v.

(7) Belmabkhout, Y.; Serna-Guerrero, R.; Sayari, A. Amine-bearing mesoporous silica for CO2 removal from dry and humid air. *Chem. Eng. Sci.* **2010**, *65* (11), 3695−3698, DOI: 10.1016/j.ces.2010.02.044.

(8) Choi, S.; Gray, M. L.; Jones, C. W. Amine-tethered solid adsorbents coupling high adsorption capacity and regenerability for CO2 capture from ambient air. *ChemSusChem* **2011**, *4* (5), 628−635, DOI: 10.1002/cssc.201000355.

(9) Choi, S.; Drese, J. H.; Eisenberger, P. M.; Jones, C. W. Application of amine-tethered solid sorbents for direct CO2 capture from the ambient air. *Environ. Sci. Technol.* **2011**, *45* (6), 2420−2427, DOI: 10.1021/es102797w.

(10) Chaikittisilp, W.; Lunn, J. D.; Shantz, D. F.; Jones, C. W. Poly(L-lysine) brush-mesoporous silica hybrid material as a biomolecule-based adsorbent for CO2 capture from simulated flue gas and air. *Chem.—Eur. J.* **2011**, *17* (38), 10556−10561, DOI: 10.1002/chem.201101480.

(11) Stuckert, N. R.; Yang, R. T. CO2 capture from the atmosphere and simultaneous concentration using zeolites and amine-grafted SBA-15. *Environ. Sci. Technol.* **2011**, *45* (23), 10257−10264, DOI: 10.1021/Es202647a.

(12) Goeppert, A.; Czaun, M.; May, R. B.; Prakash, G. K. S.; Olah, G. A.; Narayanan, S. R. Carbon dioxide capture from the air using a polyamine based regenerable solid adsorbent. *J. Am. Chem. Soc.* **2011**, *133* (50), 20164−20167, DOI: 10.1021/Ja2100005.

(13) Chueh, W. C.; Falter, C.; Abbott, M.; Scipio, D.; Furler, P.; Haile, S. M.; Steinfeld, A. High-flux solar-driven thermochemical dissociation of CO2 and H2O using nonstoichiometric ceria. *Science* **2010**, *330* (6012), 1797−1801, DOI: 10.1126/science.1197834.

(14) Loutzenhiser, P. G.; Meier, A.; Steinfeld, A. Review of the two-step H2O/CO2-splitting solar thermochemical cycle based on Zn/ZnO redox reactions. *Materials* **2010**, *3* (11), 4922−4938, DOI: 10.3390/ma3114922.

(15) Graves, C.; Ebbesen, S. D.; Mogensen, M.; Lackner, K. S. Sustainable hydrocarbon fuels by recycling CO2 and H2O with renewable or nuclear energy. *Renewable Sustainable Energy Rev.* **2011**, *15* (1), 1−23, DOI: 10.1016/j.rser.2010.07.014.

(16) Zeman, F. S.; Keith, D. W. Carbon neutral hydrocarbons. *Philos. Trans. R. Soc., A* **2008**, *366* (1882), 3901−3918, DOI: 10.1098/rsta.2008.0143.

(17) Olah, G. A.; Prakash, G. K. S.; Goeppert, A. Anthropogenic chemical carbon cycle for a sustainable future. *J. Am. Chem. Soc.* **2011**, *133* (33), 12881−12898, DOI: 10.1021/Ja202642y.

(18) Realff, M. J.; Eisenberger, P. Flawed analysis of the possibility of air capture. *Proc. Natl. Acad. Sci. U.S.A.* **2012**, *109*, (25); DOI: 10.1073/pnas.1203618109.

(19) Socolow, R.; Desmond, M.; Aines, R.; Blackstock, J.; Bolland, O.; Kaarsberg, T.; Lewis, N.; Mazzotti, M.; Pfeffer, A.; Sawyer, K.; Siirola, J.; Smit, B.; Wilcox, J. *Direct Air Capture of CO2 with Chemicals*; American Physical Society (APS): 2011.

(20) House, K. Z.; Baclig, A. C.; Ranjan, M.; van Nierop, E. A.; Wilcox, J.; Herzog, H. J. Economic and energetic analysis of capturing CO2 from ambient air. *Proc. Natl. Acad. Sci. U.S.A.* **2011**, *108* (51), 20428−20433, DOI: 10.1073/pnas.1012253108.

(21) Herzog, H. J.; House, K. Z.; Baclig, A. C.; Nierop, E. A. v.; Wilcox, J. Reply to Realff and Eisenberger: energy requirements of air capture systems. *Proc. Natl. Acad. Sci. U.S.A.* **2012**, *109*, (25); DOI: 10.1073/pnas.1204448109

(22) Furler, P.; Scheffe, J. R.; Steinfeld, A. Syngas production by simultaneous splitting of H2O and CO2 via ceria redox reactions in a high-temperature solar reactor. *Energy Environ. Sci.* **2012**, *5* (3), 6098−6103, DOI: 10.1039/C1ee02620h.

(23) Elimelech, M.; Phillip, W. A. The future of seawater desalination: energy, technology, and the environment. *Science* **2011**, *333* (6043), 712−717, DOI: 10.1126/science.1200488.
(24) Schladt, M. J.; Filburn, T. P.; Helble, J. J. Supported amine sorbents under temperature swing absorption for CO2 and moisture capture. *Ind. Eng. Chem. Res.* **2007**, *46* (5), 1590−1597, DOI: 10.1021/ie0608915.
(25) Belmabkhout, Y.; Serna-Guerrero, R.; Sayari, A. Adsorption of CO2-containing gas mixtures over amine-bearing pore-expanded MCM-41 silica: application for gas purification. *Ind. Eng. Chem. Res.* **2010**, *49* (1), 359−365, DOI: 10.1021/ie900837t.
(26) Chaikittisilp, W.; Khunsupat, R.; Chen, T. T.; Jones, C. W. Poly(allylamine)-mesoporous silica composite materials for CO2 capture from simulated flue gas or ambient air. *Ind. Eng. Chem. Res.* **2011**, *50* (24), 14203−14210, DOI: 10.1021/Ie201584t.
(27) Chaikittisilp, W.; Kim, H. J.; Jones, C. W. Mesoporous alumina-supported amines as potential steam-stable adsorbents for capturing CO2 from simulated flue gas and ambient air. *Energy Fuels* **2011**, *25* (11), 5528−5537, DOI: 10.1021/Ef201224v.
(28) Gebald, C.; Wurzbacher, J. A.; Tingaut, P.; Zimmermann, T.; Steinfeld, A. Amine-based nanofibrillated cellulose as adsorbent for CO2 capture from air. *Environ. Sci. Technol.* **2011**, *45* (20), 9101−9108, DOI: 10.1021/Es202223p.
(29) McDonald, T. M.; Lee, W. R.; Mason, J. A.; Wiers, B. M.; Hong, C. S.; Long, J. R. Capture of carbon dioxide from air and flue gas in the alkylamine-appended metal-organic framework mmen-Mg-2(dobpdc). *J. Am. Chem. Soc.* **2012**, *134* (16), 7056−7065, DOI: 10.1021/ja300034j.
(30) Choi, S.; Watanabe, T.; Bae, T. H.; Sholl, D. S.; Jones, C. W. Modification of the Mg/DOBDC MOF with amines to enhance CO2 adsorption from ultradilute gases. *J. Phys. Chem. Lett.* **2012**, *3* (9), 1136−1141, DOI: 10.1021/jz300328j.
(31) Bollini, P.; Didas, S. A.; Jones, C. W. Amine-oxide hybrid materials for acid gas separations. *J. Mater. Chem.* **2011**, *21* (39), 15100−15120, DOI: 10.1039/C1jm12522b.
(32) Li, W.; Choi, S.; Drese, J. H.; Hornbostel, M.; Krishnan, G.; Eisenberger, P. M.; Jones, C. W. Steam-stripping for regeneration of supported amine-based CO2 adsorbents. *ChemSusChem* **2010**, *3* (8), 899−903, DOI: 10.1002/cssc.201000131.
(33) Wurzbacher, J. A.; Gebald, C.; Steinfeld, A. Separation of CO2 from air by temperature-vacuum swing adsorption using diamine-functionalized silica gel. *Energy Environ. Sci.* **2011**, *4* (9), 3584−3592, DOI: 10.1039/C1ee01681d.
(34) Sayari, A.; Belmabkhout, Y.; Serna-Guerrero, R. Flue gas treatment via CO2 adsorption. *Chem. Eng. J.* **2011**, *171* (3), 760−774, DOI: 10.1016/j.cej.2011.02.007.
(35) Wang, L. F.; Yang, R. T. Increasing selective CO2 adsorption on amine-grafted SBA-15 by increasing silanol density. *J. Phys. Chem. C* **2011**, *115* (43), 21264−21272, DOI: 10.1021/Jp206976d.
(36) Serna-Guerrero, R.; Da'na, E.; Sayari, A. New Insights into the Interactions of CO2 with amine-functionalized silica. *Ind. Eng. Chem. Res.* **2008**, *47* (23), 9406−9412, DOI: 10.1021/ie801186g.
(37) Bacsik, Z.; Ahlsten, N.; Ziadi, A.; Zhao, G. Y.; Garcia-Bennett, A. E.; Martin-Matute, B.; Hedin, N. Mechanisms and kinetics for sorption of CO2 on bicontinuous mesoporous silica modified with n-propylamine. *Langmuir* **2011**, *27* (17), 11118−11128, DOI: 10.1021/La202033p.
(38) Knofel, C.; Martin, C.; Hornebecq, V.; Llewellyn, P. L. Study of carbon dioxide adsorption on mesoporous aminopropylsilane-functionalized silica and titania combining microcalorimetry and in situ infrared spectroscopy. *J. Phys. Chem. C* **2009**, *113* (52), 21726−21734, DOI: 10.1021/Jp907054h.
(39) Danon, D.; Stair, P. C.; Weitz, E. FTIR study of CO2 adsorption on amine-grafted SBA-15: elucidation of adsorbed species. *J. Phys. Chem. C* **2011**, *115* (23), 11540−11549, DOI: 10.1021/Jp200914v.
(40) Pinto, M. L.; Mafra, L.; Guil, J. M.; Pires, J.; Rocha, J. Adsorption and activation of CO2 by amine-modified nanoporous materials studied by solid-state NMR and (13)CO2 adsorption. *Chem. Mater.* **2011**, *23* (6), 1387−1395, DOI: 10.1021/Cm1029563.
(41) Satyapal, S.; Filburn, T.; Trela, J.; Strange, J. Performance and properties of a solid amine sorbent for carbon dioxide removal in space life support applications. *Energy Fuels* **2001**, *15* (2), 250−255, DOI: 10.1021/ef0002391.
(42) Belmabkhout, Y.; De Weireld, G.; Sayari, A. Amine-bearing mesoporous silica for CO2 and H2S removal from natural gas and biogas. *Langmuir* **2009**, *25* (23), 13275−13278, DOI: 10.1021/la903238y.
(43) Serna-Guerrero, R.; Belmabkhout, Y.; Sayari, A. Triamine-grafted pore-expanded mesoporous silica for CO2 capture: effect of moisture and adsorbent regeneration strategies. *Adsorption* **2010**, *16* (6), 567−575, DOI: 10.1007/s10450-010-9253-y.
(44) Li, G.; Xiao, P.; Webley, P. Binary adsorption equilibrium of carbon dioxide and water vapor on activated alumina. *Langmuir* **2009**, *25* (18), 10666−10675, DOI: 10.1021/la901107s.
(45) Belbekhouche, S.; Bras, J.; Siqueira, G.; Chappey, C.; Lebrun, L.; Khelifi, B.; Marais, S.; Dufresne, A. Water sorption behavior and gas barrier properties of cellulose whiskers and microfibrils films. *Carbohydr. Polym.* **2011**, *83* (4), 1740−1748, DOI: 10.1016/j.carbpol.2010.10.036.
(46) Ahn, H.; Lee, C. H. Effects of capillary condensation on adsorption and thermal desorption dynamics of water in zeolite 13X and layered beds. *Chem. Eng. Sci.* **2004**, *59* (13), 2727−2743, DOI: 10.1016/j.ces.2004.04.011.
(47) Al-Muhtaseb, A. H.; McMinn, W. A. M.; Magee, T. R. A. Water sorption isotherms of starch powders - Part 1: mathematical description of experimental data. *J. Food Eng.* **2004**, *61* (3), 297−307, DOI: 10.1016/S0260-8774(03)00133-X.
(48) Iglesias, H. A.; Chirife, J. Isosteric heats of water vapor sorption on dehydrated foods part I. analysis of the differential heat curves. *Lebensmittel-Wissenschaft Technol.* **1976**, *9* (2), 116−122.